3.9.4.4. *Matrix flushing*

Once the correct value of RIR is determined for each phase, the matrix-flushing method can be applied using equation (3.9.15). For fluorite in sample 1D, the calculation proceeds as follows:

$$W_{\text{fluorite}} = \frac{I_{\text{fluorite}}/\text{RIR}_{\text{fluorite}}}{\sum_{k=1}^{n} I_k/\text{RIR}_{ks}} = \frac{6559.6/3.617}{474.5/1.0 + 6559.6/3.617 + 5468.5/4.856} = 0.5312, \quad (3.9.33)$$

compared with a value of 0.5358 added to the sample by weight. Fig. 3.9.4 shows the bias for fluorite in all samples analysed by the matrix-flushing method. Once again, there is good agreement between the weighed and analysed amounts. However, it is worth reiterating that this method normalizes the sum of all analysed weight fractions to unity. If amorphous or non-analysed phases are present in the sample, then the weight fractions will be overestimated relative to their absolute abundances.

3.9.4.5. *Rietveld-based methods*

The strengths and weaknesses of some of the methods described in Section 3.9.3 are highlighted through a study of the mechanism and kinetics of nucleation and crystal growth in the context of the Bayer process for the extraction of aluminium from bauxite ores (Webster *et al.*, 2010). Specifically, the experiments utilize synthetic Bayer liquors, consisting of Al-loaded caustic solutions to which a variety of seed material is added. Several polymorphs of $Al(OH)_3$ (gibbsite, bayerite and nordstrandite) crystallize from solution onto the seed material. The rate of crystallization and the ratio of the phases formed depend on the sample conditions used, including the Al and caustic concentrations in solution, as well as sample temperature.

The mechanism and rate of crystallization were followed by collecting XRD data at the powder-diffraction beamline of the Australian Synchrotron[4] over a period of about 3 h. The diffractometer incorporates a Mythen detector (Schmitt *et al.*, 2003) which allows for the simultaneous collection of 80° 2θ of the diffraction pattern. A wavelength of 0.826 Å was used to ensure adequate penetration of the beam in the sample. The sample environment (Madsen *et al.*, 2005; Norby *et al.*, 1998) consisted of a 1-mm quartz glass capillary containing a slurry of the seed and Bayer liquor heated to temperatures between 333 and 348 K using a hot-air blower.

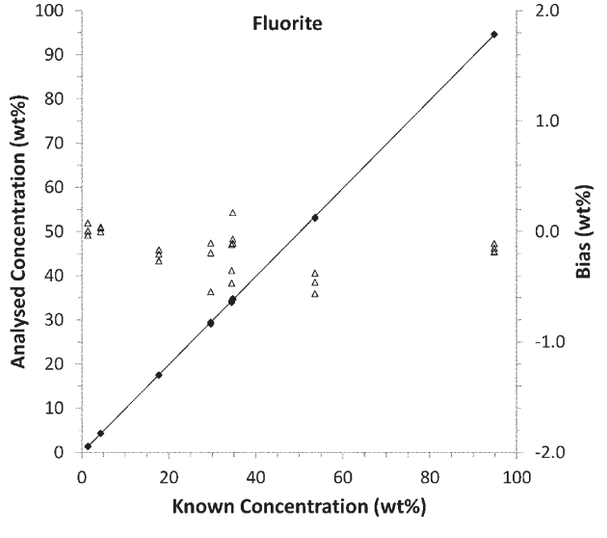

Figure 3.9.4
Plot of the analysed concentration (black diamonds – left axis) and the bias (open triangles – right axis) expressed as wt% for fluorite using the matrix-flushing method with RIRs of 1.0, 3.617 and 4.856 for corundum, fluorite and zincite, respectively. The RIRs were determined using sample 1H where the corundum, fluorite and zincite concentrations are 35.12, 34.69 and 30.19 wt%, respectively.

The data were analysed using *TOPAS* (Bruker AXS, 2013), where a learned-profile approach to peak modelling was used with an empirical instrument width and shape contribution determined using the NIST SRM660 LaB_6 profile standard. For the samples in the study, refined parameters included 2θ zero offset, a Chebychev polynomial pattern background and, for each phase, the Rietveld scale factor, crystallite size and strain, and unit-cell dimensions.

A number of different approaches were used to extract the phase abundances at each stage of the reaction. Initially, QPA was derived using equation (3.9.26); the value that many Rietveld analysis programs output as their first estimate of phase abundance. Fig. 3.9.5 shows the QPA output from an *in situ* experiment in which goethite (FeOOH) was added as the seed.

At the start of the experiment, prior to the crystallization of any of the $Al(OH)_3$ polymorphs, Fig. 3.9.5 shows that the reported concentration of the goethite seed is 100 wt% since it is the only phase represented in the analysis at that time. On formation of gibbsite, bayerite and nordstrandite, the goethite concentration appears to decrease progressively to about 65 wt% while the total $Al(OH)_3$ concentration reaches about 35 wt% at the end of the experiment. However, these figures are in disagreement with (i) the fact that goethite is unlikely to dissolve or otherwise be consumed in this system (Murray *et al.*, 2009), (ii) the known addition of goethite to the sample (14.13 wt%) and (iii) the total amount of $Al(OH)_3$ available from solution (15.92 wt%). The problem with the QPA in this case arises from the fact that only the crystalline components are considered in the analysis and that equation (3.9.26) normalizes the sum of their analysed weight fractions to unity. However, aluminium, which is in solution at the start of the run, forms crystalline phases continuously throughout the reaction after an initial induction period. In order to overcome the anomalies in the QPA results, it is necessary to consider the sample as a whole; that is, the concentration of both the solid and liquid components in the X-ray beam for the duration of the experiment.

In this sample, the concentration of the goethite seed was 14.13 wt% in the slurry injected into the sample capillary. If the assumption is made that, in this environment, goethite is unreactive and its concentration will not change during the reaction, it can be used as an internal standard to put the $Al(OH)_3$ concentrations on an absolute basis. The QPA results derived using the internal standard or 'spiked' approach in equation (3.9.25) are shown in Fig. 3.9.6.

The goethite concentration is fixed at the known addition (14.13 wt%) at the start of the experiment. However, the concentrations of the $Al(OH)_3$ polymorphs are now put on an absolute scale, thus allowing derivation of more meaningful reaction mechanisms.

If, however, there is residual doubt about the reactivity of the goethite, it may be necessary to use the external standard approach embodied in equation (3.9.21). In this case, the value for the instrument constant, K, can be derived using the Rietveld scale factor, ZMV and the known addition of goethite in a

[4] Australian Synchrotron beamtime award number AS091/PD1035.